

# Tracking and Predicting COVID-19 Epidemic in China Mainland

Haoxuan Sun<sup>1</sup>, Yumou Qiu<sup>2</sup>, Han Yan<sup>3</sup>, Yaxuan Huang<sup>4</sup>, Yuru Zhu<sup>5</sup> and  
Song Xi Chen<sup>6</sup>

*Communications on the research work can be made with S.X. Chen at  
csx@gsm.pku.edu.cn*

---

## Abstract

By proposing a varying coefficient Susceptible-Infected-Removal model (vSIR), we track the epidemic of COVID-19 in 30 provinces in China and 15 cities in Hubei province, the epicenter of the outbreak. It is found that the spread of COVID-19 has been significantly slowing down within the two weeks from January 27 to February 10th with 87.0% and 84.3% reductions in the reproduction number  $R_0$  among the 30 provinces and 15 Hubei cities, respectively. This suggests the extreme control measures implemented since January 23, which include cutting off Wuhan and many other cities and towns, a great public awareness and high level of self isolation at home, have contributed to a substantial decline in the reproductivity of the COVID-19 in China. We predict that Hubei province will reach its peak between February 20 and 22, 2020, and if the removal rate can be increased to 0.1, the epidemic outside Hubei province will end in May 2020, and inside Hubei in early June.

*Keywords:* Basic reproductive rate; Bootstrap prediction inference; COVID-19; SIR model; Varying coefficient model;

---

<sup>1</sup>Big Data Research Institute, Peking University

<sup>2</sup>Department of Statistics, Iowa State University; Corresponding Author

<sup>3</sup>School of Mathematical Sciences, Sichuan University

<sup>4</sup>Yuanpei College, Peking University

<sup>5</sup>Center for Statistical Science, Peking University

<sup>6</sup>Guanghua School of Management and Center for Statistical Science, Peking University; Corresponding Author.

## 1 1. Introduction

2 The Corona Virus Disease 2019 (COVID-19) has created a profound public health emergency in China and has spread to 25 countries so far [1]. It has become an epidemic with more than 71,000 confirmed infections and 3 1,775 reported deaths worldwide as on February 17 2020. The COVID-19 is caused by a new corona viruses that is genetically similar to the viruses 4 causing severe acute respiratory syndrome (SARS) and Middle East respiratory syndrome (MERS). Despite a relatively lower fatality rate comparing 5 to SARS and MERS, the COVID-19 spreads faster and infects much more people than the SARS-03 outbreak. 6

7 The city of Wuhan, the origin of the outbreak, has been locked up to curtail population movement since January 23 in an effort to stop the spread 8 of the epidemic, followed by more than 50 prefecture level cities (as on 8th of February) and countless number of towns and villages in China. A high 9 percentage of the population are exercising self-isolation in their homes. The spring festival holiday period had been extended with all schools and uni- 10 versities closed and all students staying where they are indefinitely. The country is virtually in a stand-still, and the economy and people's livelihood 11 have been severely affected by the epidemic. 12

13 There is an urgent need to assess the speed of the disease transmission and to check if the existing containment measures have successfully slowed 14 down the spread of the disease or not. The Susceptible-Infected-Removal (SIR) model [2] and its generalizations, for instance the SEIR model [3] with 15 four or more compartments are commonly used to model the dynamics of infectious disease outbreaks. See [4, 5, 6, 7] for statistical estimation and 16 inference for stochastic versions of the SIR model. SEIR models have been used to produce early results on COVID-19 in [8, 9, 10], which produced 17 the first three estimates of the all important basic reproduction number  $R_0$ : 2.68 by [8], 3.81 by [9] and 6.47 by [10]. The  $R_0$  is the expected number 18 of infections by one infectious person during the course of his/her infectious period, and is a key measure of an epidemic. If  $R_0 < 1$ , the epidemic will die 19 down eventually with the speed of the decline depends on how small  $R_0$  is; otherwise, the epidemic will explode until it runs out of its course. 20

21 The SEIR models that was employed in the above three cited works for the COVID-19 assume constant model coefficients, implying a constant regime 22 of transmission during the course of the epidemic. This is too idealistic for modeling COVID-19 as it cannot reflect the intervention measures by the 23 24 25 26 27 28 29 30 31 32 33 34 35 36 37

38 authorities and the citizens, which should have made the infectious rate ( $\beta$ )  
39 and the reproduction number ( $R_0$ ) varying with respect to the time.

40 To reflect the changes due to the strong government intervention and  
41 self protection, we propose a varying coefficient SIR (vSIR) model, which  
42 can capture the varying dynamics of the epidemic. The vSIR model is easy  
43 to be implemented via the locally weighted regression approach [11] that  
44 produces estimates with desired smoothness, and yet is able to capture the  
45 changing dynamics of COVID-19's reproduction, with guaranteed statistical  
46 consistency and needed standard errors. The consistent estimator and its  
47 confidence interval are needed for estimating the trend of  $R_0$ , assessing the  
48 effectiveness of infection control ( $R_0$  is significantly less than 1 continuously  
49 for 7 days), and predicting the final number of infection cases and the future  
50 epidemic trend.

## 51 2. Results

52 By applying the vSIR model, we produce daily estimates of the infectious  
53 rate  $\beta(t)$  and the reproduction number  $R_0(t)$  ( $t$  denotes time) for 30 provinces  
54 and 15 major cities (including Wuhan) in Hubei province from January 21  
55 or a later date between January 24-29 depending on the first confirmed case  
56 to February 10. We report standard error in the parentheses following the  
57 estimate.

### 58 2.1. Main findings

- 59 • Despite the total number of confirmed cases and the death are increas-  
60 ing, the spread of COVID-19 has shown a great slowing down in China  
61 within the two weeks from January 27 to February 10 as shown by  
62 88.0% and 86.8% reductions in the reproduction number  $R_0$  among the  
63 30 provinces and the 15 cities in Hubei, respectively.
- 64 • The average  $R_0^{14}$  (based on 14-day infectious duration) on January 27th  
65 was 6.42 (1.57) and 7.67 (2.46), respectively, for the 27 provinces and  
66 the 7 Hubei cities with confirmed cases by January 23rd. One week  
67 later on February 3rd, the  $R_0^{14}$  was averaged at 2.39 (0.70) for the 30  
68 provinces and 2.94 (0.56) for the 15 Hubei cities, representing 62.8%  
69 and 61.7% reductions, respectively, over the 7 days. On February 10th,  
70 the average  $R_0^{14}$  dropped further to 0.77 (0.33) for the 30 provinces and  
71 1.01 (0.43) for the 15 Hubei cities, which were either below or close to  
72 the critical threshold level 1.

- 73 ● The profound slowing down in the reproductivity of COVID-19 can  
74 be attributed to a series of action and measures by the government  
75 and the public, which include cutting off Wuhan and other cities from  
76 January 23, a rapid public awareness of the epidemic and the extensive  
77 self protection taken and high level of self isolation at home exercised  
78 over a much extended Spring Festival holiday period.
- 79 ● There are increasing numbers of provinces and cities in Hubei whose  
80 14-day  $R_0$  has been statistically below 1, as detailed in Table 1, which  
81 would foreshadow the coming of the turning point for containment of  
82 the epidemic, if the control measures implemented since January 23  
83 can be continued.
- 84 ● If the current decreasing trend of  $R_0$  continues, Hubei will reach peak  
85 infection between February 20 and February 22. Many non-Hubei  
86 provinces have already reached the peak. If the recovery rate can be  
87 increased to 0.1 meaning the average recover time is 10 days after diag-  
88 nosis, the number of infected patients  $I(t)$  will be dramatically reduced  
89 in March, and the epidemic will end in early June; see Figure 3.
- 90 ● The eventual control of COVID-19 is rested on if the existing control  
91 measures can be continued further for a period of time. The biggest  
92 challenges that can jeopardize the great effort from late January are  
93 from the impatient populations eager to get out of the self-isolation  
94 driven by either economic needs (migrant workers eager to coming back  
95 to cities for income) or people trying to escape from the boredom of  
96 self isolation while encouraged by the declining infections in the last  
97 two weeks.
- 98 ● The implications of China's experience in combating COVID-19 to  
99 other countries facing the epidemic are two folds. One is to reduce the  
100 person-to-person contact rate by self isolation and curtailing of popu-  
101 lation movement; another is to reduce the transmission probability by  
102 wearing protective wears should a contact has to be made.

## 103 2.2. Basic reproduction number

104 At a date  $t$ , the reproduction number based on an average infectious  
105 duration  $D$  is  $R_0^D(t) = \beta(t)D$  where  $\beta(t)$  is the daily infection rate at  $t$ . We  
106 do not adopt the version involving  $\gamma$ , the removal rate, since its estimation

107 is highly volatile at the early stage of an epidemic. A general version of  
108  $R_0(t)$  may be defined as  $\int_{t-D_1}^{t+D_2} \beta(u)du$  where positive  $D_1$  and  $D_2$  represent  
109 the infectious durations before and after diagnosis, respectively. The  $R_0^D(t)$   
110 given above can be viewed as an approximation by the Middle Value Theorem  
111 in calculus with  $D = D_1 + D_2$ .

112 Research works [12, 13, 14] so far on COVID-19 have informed a range of  
113 duration for incubation, from onset of illness to diagnosis and then to hos-  
114 pitalization. The average incubation period from the three studies ranged  
115 from 3.0 to 5.2 days; the median duration from onset to diagnosis was 4  
116 days [13]; and the mean duration from onset to first medical visit and then  
117 to hospitalization were 4.6 and 9.1 days [12], respectively. Based on a data  
118 sample of 391 cases from Shenzhen, the average incubation period was 4.46  
119 (0.26) days and the average duration from onset to hospitalization were 3.9  
120 (0.19) days, respectively, where standard error is reported in the parenthe-  
121 ses. Another dataset of 100 confirmed cases in Shaoyang (Hunan Province)  
122 revealed the average durations from onset to diagnosis and from diagnosis  
123 to discharge were 5.67 (0.39) and 10.12 (0.43) days, respectively. There is  
124 a recent revelation [13] that asymptomatic patients can be infectious, which  
125 would certainly prolong the infectious duration.

126 There are much variation in the medical capability in timely diagnosis and  
127 hospitalization (thus quarantine) of the infected across the country. Thus,  
128 the infectious duration  $D$  would vary among the provinces and cities, and  
129 would change with respect to the stage of the epidemic as well.

130 Given the diverse range of infectious duration across the provinces and  
131 cities, in order to standardize and make the reproduction number  $R_0$  readily  
132 comparable, we calculated the  $R_0^D$  based on three levels of  $D$ : 7, 10.5 and  
133 14 days, which represent three scenarios of responsiveness in diagnosing,  
134 hospitalization and hence quarantine of the infected. Calculation of the  $R_0$   
135 at other duration can be made by inflating or deflating a  $R_0^D$  proportionally  
136 to reflect a local reality.

### 137 2.3. Reproductivity of COVID-19

138 Figures 1 presents the time series of  $R_0^D(t)$  at the three levels of  $D$  for  
139 the 30+15 provinces/cities from late January to February 11th. Figure 2  
140 displays three cross sectional  $R_0^{14}$  and their confidence intervals on January  
141 27th, February 3rd and 10th, respectively.

142 Figure 1 reveals a monotone decreasing trend for almost all the provinces  
143 and cities with only exceptions for Hubei, Guizhou, Jinlin, Neimenggu and

144 Qinghai. Even for those exceptional provinces, the recent trend is largely de-  
145 clining. The non-monotone pattern for non-Hubei provinces were largely due  
146 to relative small number of infected cases and waves of introduced infections.  
147 However, the one for Hubei and Wuhan suggests low data quality and in par-  
148 ticularly under reporting and reporting delay. The epidemic statistics from  
149 Hubei and the city of Wuhan before January 21th were severely incomplete  
150 and with irregular patterns. This was the reason we start Hubei's analysis  
151 from January 21th.

152 The average  $R_0^{14}(t)$  among the 27 provinces (with confirmed cases on and  
153 prior to January 23rd) was 6.42 (1.57), and 7.67 (2.46) for 7 of the 15 Hubei  
154 cities on January 27. These levels were comparable to the level of  $R_0$  (6.47)  
155 given in [10].

156 One week later on February 3rd,  $R_0^{14}$  was averaged at 2.39 (0.70) for the  
157 30 provinces and 2.94 (0.56) for the 15 Hubei cities, indicating that cutting  
158 off Wuhan and other cities, and the start of wearing face masks and self  
159 isolation at home from January 23th had contributed to 62.8% and 61.7%  
160 reduction in the  $R_0$ . In the following week starting from February 4th, the  
161 average  $R_0^{14}$  came down to 0.77 (0.33) for the 30 provinces and 1.01 (0.43) for  
162 the 15 Hubei cities on February 10th, representing further 67.8% and 65.6%  
163 reductions, respectively, during the second week. This reflects the beneficial  
164 effects of the continued large scale self-isolation within the extended spring  
165 festival holiday period.

166 Table 1 provides the reproduction number  $R_0^D$  at the three durations  
167 on February 10th. It shows that 5 provinces and 4 Hubei cities'  $R_0^{14}$  were  
168 significantly above 1 (at 5% significance level). There are 17 provinces and  
169 8 Hubei cities'  $R_0^{14}$  were significantly below 1, which were 4 and 6 more  
170 than those a day earlier on February 9th, and 9 and 8 more than those on  
171 February 8th, respectively. If we use the shorter  $D = 10.5$ , 27 provinces  
172 and 11 Hubei cities have been significantly below 1 for 1-7 consecutive days.  
173 These indicate that the reproduction number  $R_0$  has showed signs of crossing  
174 below the critical threshold 1 in increasing number of provinces and cities  
175 in Hubei around February 8-10. An updated Table 1 for February 16th are  
176 available in Table A1 in the Supplementary Information (SI), which shows  
177 continued improvement since February 10.

178 Given the significant decline in the reproduction numbers, it is time to  
179 discuss the turning point for COVID-19 for China. If a province or city's  $R_0^D$   
180 starts to be below 1 significantly (at 5% level), we would say the province  
181 or city have showed signs of the turning point. Given the uncertainty with

182 the data records, especially those large variation in daily infected numbers  
183 coming out of Wuhan and Hubei, the turning point of the epidemic would  
184 be confirmed if  $R_0^D$  have been significantly below 1 for  $D_1$  days, where  $D_1$   
185 is the period of infection before diagnosis, assuming all diagnosed can be  
186 quarantine immediately. Based on the results in [12, 13, 14],  $D_1 = 7$  may be  
187 considered. Then, some of the 30+15 provinces/cities have already reached  
188 the turning point, and more will be so in the coming days according to latest  
189 Table A1 in SI.

#### 190 2.4. Prediction

191 Based on the estimated  $\beta(t)$  over time, we predict COVID-19's future tra-  
192 jectories as solutions to the vSIR model. We consider two scenarios for the  
193 recovery rate  $\gamma$ . One uses the empirical estimate based on data to February  
194 13th. As an effective cure for the virus has not been found, the estimated  
195 recovery rates are quite low. Among the provinces with more than 100 in-  
196 fections on February 13, Hunan had the highest recovery rate 0.06, followed  
197 by Jilin and Zhejiang (0.05), and then Tianjin, Chongqing, Hebei, Guizhou,  
198 Henan and Shanghai (0.046–0.049). Hubei, the province at the center of the  
199 epidemic, was 0.021. The other scenario is to choose  $\gamma = 0.1$ , which means  
200 the average removal time from diagnosis is 10 days, representing improvement  
201 in the treatment for COVID-19 patients as time progress.

202 Tables 2 and 3 present the 95% prediction intervals for the peak and end  
203 times of the number of infections (subtracted by the number of removals),  
204 and the cumulative number of infected at the ending based on the two sce-  
205 narios of the recovery rate, respectively. We use data to February 13 2020 for  
206 the prediction. The predicted infection number  $\hat{I}(t)$  is within 5% and 10%  
207 deviation from its observed value on February 14 and February 15, 16 respec-  
208 tively; see Table A2 in SI for the detailed prediction error. The prediction  
209 based on the most recent data to February 16 gives similar results.

210 From Table 2, with the estimated recovery rate, Hubei will reach peak in-  
211 fection between February 20 and February 22. For many non-Hubei provinces,  
212 their peak time have already occurred as early as February 4 (Qinghai),  
213 February 7 (Zhejiang) and February 9 (Guangdong, Shanghai, Henan, Jilin,  
214 Gansu), and five other provinces on February 10. The last row gives the  
215 predictions for all the non-Hubei provinces combined, which reaches peak  
216 infection between February 10th and 17th with 95% confidence.

217 From the trajectory of the vSIR model, the epidemic will end in late  
218 October 2020 for the non-Hubei provinces with the accumulated number of



219 final infected cases in the range 17,894–19,163. The total non-Hubei infected  
220 number was 11,977 (as February 13). The ending time of Hubei is predicted  
221 to be March 2021 with final infected in the range 83,972–92,103. The current  
222 total infected cases in Hubei was 52,388 on February 13th.

223 It should be highlighted that the above prediction results were based on  
224 the estimated recovery rate so far. Table 3 gives the results with the recovery  
225 rate increased to 0.1. The trajectories of  $I(t)$  under the proposed vSIR model  
226 with the estimated recovery rate and  $\gamma = 0.1$  are presented in Figure 3. With  
227 a higher recovery rate of 0.1, the duration of the epidemic will be shorten  
228 substantially. Figure 3 indicates that the number of infected will quickly  
229 decrease in late February and March with very few cases left in April. The  
230 ending time for Hubei will be brought early to June 2020 with total number of  
231 infection reduced to the range 69,896–73,460, down by 14,076–18,643. Most  
232 of the non-Hubei provinces will end in April, 2020. Some provinces with few  
233 number of total infected cases may end as early as March (Qinghai, Jilin,  
234 Neimenggu). This shows that improving the recovery rate is an efficient way  
235 to end the COVID-19 infection early given the current decreasing trend of  
236  $\beta(t)$ , as it leads to the reduction of the infectious duration.

### 237 3. Methods

238 Let  $S(t)$ ,  $I(t)$  and  $R(t)$  be the counts of susceptible, infected and recovered  
239 (including dead) persons in a given city or province at time  $t$ , respectively.  
240 Let  $N$  be the total population of the city/province. We propose a vary-  
241 ing coefficient Susceptible-Infected-Recovered (vSIR) model to estimate the  
242 dynamics of COVID-19 and predict its future course of spread.

#### 243 3.1. Data

244 The daily records of infected, dead and recovered patients released by  
245 National Health Commission of China (NHCC) are obtained from the NHCC  
246 website, with the first confirmed record for Wuhan on December 8th, 2019,  
247 followed by 30 provinces in mainland China and 15 cities in Hubei province  
248 where Wuhan is the capital city. We did not consider data from Tibet due  
249 to very small number of cases. Table A3 in SI provides the starting dates  
250 of the data records and analysis for each province and city. Due to severe  
251 under-reporting in the first 39 days of the epidemics in Wuhan and Hubei, we  
252 consider data from January 16th for Wuhan and Hubei. For other provinces  
253 and Hubei cities, the starting dates for data are those of first confirmed



254 case, and the analysis date started four days afterward due to the estimation  
255 approach for estimating the infectious rate  $\beta(t)$ . The latest start for analysis  
256 was January 29th for Qinghai province and three cities in Hubei province.  
257 The second last date was January 28th that started 2 provinces and 5 Hubei  
258 cities.

259 The data from *Shenzhen Government Online* are epidemic statistics re-  
260 leased by the Shenzhen Municipal Health Commission from January 19th to  
261 February 13th [15]. One dataset about the details of confirmed cases con-  
262 tains the time of onset, time of hospital admission, cause of illness and other  
263 information of 391 cases, including 188 males and 203 females. The admis-  
264 sion time of these cases ranged from January 9th to February 11th. The  
265 other dataset reports the discharge time for 94 cases in the former dataset.  
266 Besides, the dataset of 100 confirmed cases was released by the Shaoyang  
267 Municipal Health Committee [16] on February 14 that includes 48 males and  
268 52 females with the onset dates ranging from January 12 to February 11.

### 269 3.2. Time-varying coefficient SIR model

270 The Susceptible-Infective-Removal (SIR) model [2] is a commonly used  
271 epidemiology model for the dynamic of susceptible  $S(t)$ , infected  $I(t)$  and  
272 recovered  $R(t)$  as a system of ordinary differential equations (ODEs). Here  
273 we consider a more generalized version of the SIR model in that the infectious  
274 rate  $\beta$  and the removal rate  $\gamma$  may change with respect to time so that

$$\begin{aligned}\frac{dS(t)}{dt} &= -\beta(t)I(t)\frac{S(t)}{N}, \\ \frac{dI(t)}{dt} &= \beta(t)I(t)\frac{S(t)}{N} - \gamma(t)I(t), \\ \frac{dR(t)}{dt} &= \gamma(t)I(t),\end{aligned}\tag{1}$$

275 where  $\beta(t)$  and  $\gamma(t)$  are unknown functions of time.

276 The rationale for using a time-varying  $\beta(t)$  function, rather than a con-  
277 stant  $\beta$ , is that  $\beta(t)$  is the average rate of contact per unit time multiplied by  
278 the probability of disease transmission per contact between a susceptible and  
279 an infectious subject. Due to an increasing public awareness of the epidemic  
280 and the control measures put in place, both the transmission probability  
281 and the contact rate have been reduced due to protective wear (face mask),  
282 avoidance of close contacts and self isolation. These favors for a time-varying  
283  $\beta(t)$  are also confirmed by the sharp declined in  $R_0^D(t)$  in Figures 1 and 2.

284 The removal rate will also change over time as treatments improve over time.  
285 However, our analysis (Figure S4 in SI) shows  $\gamma(t)$  is much slowly changing  
286 for most of the provinces, which led us to treat  $\gamma(t) = \gamma$  at current stage of  
287 the outbreak.

### 288 3.3. Estimation and inference

289 The reported numbers of infected and removed cases are subject to mea-  
290 surement errors. To reduce the errors, we apply a three point moving average  
291 filter on the reported counts to obtain  $\bar{I}(t) = 0.3I(t-1) + 0.4I(t) + 0.3I(t+1)$   
292 for  $2 \leq t \leq T-1$  where  $T$  is the latest time point of observation. In our  
293 analysis,  $T$  is February 13 2020. For  $t = 1$  or  $T$ , we apply two point averaging  
294 with 7/10 weight at  $t = 1$  or  $T$ , and 3/10 for  $t = 2$  or  $T-1$ . Apply the same  
295 filtering on the recovered process  $R(t)$  and obtain  $\bar{R}(t)$ . To simplify the nota-  
296 tion, we denote the filtered data  $\bar{I}(t)$  and  $\bar{R}(t)$  as  $I(t)$  and  $R(t)$  respectively,  
297 wherever there is no confusion.

Let  $\Delta_\delta R_t = R_{t+\delta} - R_t$  for  $t = 1, \dots, T - \delta$ . From the third equation in (1), we estimate  $\gamma$  by least square fitting of  $\Delta_\delta R_t$  on  $I(t)$  without intercept. We estimate  $\beta(t) - \gamma$  by a local linear regression on  $\log\{I(t)\}$ . Let  $\hat{\gamma}$  and  $\widehat{\beta(t) - \gamma}$  be the estimators, and  $\widehat{\text{Var}}(\hat{\gamma})$  and  $\widehat{\text{Var}}(\beta(t) - \gamma)$  be their estimated variances. Their close form expressions are provided in Section S.1 in SI. Then,  $\hat{\beta}(t) = \widehat{\beta(t) - \gamma} + \hat{\gamma}$  is the estimate for the varying coefficient  $\beta(t)$  in (1). The standard error of  $\hat{\beta}(t)$  can be obtained as  $\text{SE}_\beta(t) = \{\widehat{\text{Var}}(\beta(t) - \gamma) + \widehat{\text{Var}}(\hat{\gamma})\}^{1/2}$ . The 95% confidence interval for  $\beta(t)$  can be constructed as

$$(\hat{\beta}(t) - 1.96\text{SE}_\beta(t), \hat{\beta}(t) + 1.96\text{SE}_\beta(t)). \quad (2)$$

298 In the implementation, we chose  $\delta = 2$  and  $w = 5$ . Figure S1 in SI shows  
299 that the proposed vSIR model fits the observed infected number  $I(t)$  well for  
300 30 provinces in China.

### 301 3.4. Prediction for infection rate and state variables

As  $R_0^D(t) = \beta(t) \times D$ , predicting  $\beta(t)$  is equivalent to predicting  $R_0^D(t)$ . From Figure 1 and Figure S2 in SI, we see that the overall trends of  $\beta(t)$  is decreasing. But the rate of decreasing gets smaller as time travels. To model such trend, we consider the reciprocal regression

$$\beta(t) = \frac{b}{t^n - a} + e_t \quad (3)$$

302 with error  $e_t$  and unknown parameters  $a$ ,  $b$  and  $\eta$ . The parameters  $a$ ,  $b$   
303 and  $\eta$  are estimated by minimizing the sum-of-square distance between the  
304 estimates  $\hat{\beta}(t)$  and their fitted values. Let  $\tilde{a}$ ,  $\tilde{b}$  and  $\tilde{\eta}$  be the estimated  
305 parameters, and  $\tilde{\beta}(t) = \tilde{b}/(t^{\tilde{\eta}} - \tilde{a})$  be the fitted function. Figure S3 in SI  
306 shows the reciprocal model fits  $\hat{\beta}(t)$  quite well for most of the provinces,  
307 especially those with large number of infected cases.

308 With the fitted  $\tilde{\beta}(t)$ , we project  $\{S(t), I(t), R(t)\}$  via the ODEs

$$\begin{aligned}\frac{d\hat{S}(t)}{dt} &= -\tilde{\beta}(t)\hat{I}(t)\frac{\hat{S}(t)}{N}, \\ \frac{d\hat{I}(t)}{dt} &= \tilde{\beta}(t)\hat{I}(t)\frac{\hat{S}(t)}{N} - \hat{\gamma}_T\hat{I}(t), \\ \frac{d\hat{R}(t)}{dt} &= \hat{\gamma}_T\hat{I}(t).\end{aligned}\tag{4}$$

309 where  $\hat{\gamma}_T$  is the estimated recovery rate at time  $T$  using the last five days'  
310 data. With the observed  $\{S(T), I(T), R(T)\}$  at the current time  $T$  as the  
311 initial values, numerical solutions  $\{(\hat{S}(t), \hat{I}(t), \hat{R}(t)) : T \leq t < \infty\}$  for the  
312 system (4) could be obtained using the Euler method. Then, the peak time  
313 of the number of infected cases can be predicted as  $t_{\text{peak}} = \arg \max_t \hat{I}(t)$ ,  
314 and the estimated final infected number is  $\hat{N}_{\text{final}} = \hat{R}(t_{\text{end}}) + \hat{I}(t_{\text{end}})$ , where  
315  $t_{\text{end}} = \min \{t : \hat{I}(t) < 1\}$  is the estimated ending time. The 95% prediction  
316 intervals for the peak time, end time and final infected number are obtained  
317 by bootstrap resampling method. The details of the bootstrap prediction  
318 inference is provided in Section S.2 in SI.

## 319 References

- 320 [1] World Health Organization (WHO), Situation report - 26, Avail-  
321 able at [https://www.who.int/docs/default-source/coronaviruse/](https://www.who.int/docs/default-source/coronaviruse/situation-reports/20200215-sitrep-26-covid-19.pdf)  
322 [situation-reports/20200215-sitrep-26-covid-19.pdf](https://www.who.int/docs/default-source/coronaviruse/situation-reports/20200215-sitrep-26-covid-19.pdf), 2020. [Ac-  
323 cessed February 16, 2020].
- 324 [2] W. O. Kermack, A. G. McKendrick, A contribution to the mathematical  
325 theory of epidemics, Proceedings of the royal society of london. Series A,  
326 Containing papers of a mathematical and physical character 115 (1927)  
327 700–721.

- 328 [3] H. W. Hethcote, The mathematics of infectious diseases, SIAM review  
329 42 (2000) 599–653.
- 330 [4] N. G. Becker, On a general stochastic epidemic model, Theoretical  
331 Population Biology 11 (1977) 23–36.
- 332 [5] N. G. Becker, T. Britton, Statistical studies of infectious disease in-  
333 cidence, Journal of the Royal Statistical Society: Series B (Statistical  
334 Methodology) 61 (1999) 287–307.
- 335 [6] P. S. Yip, Q. Chen, Statistical inference for a multitype epidemic model,  
336 Journal of statistical planning and inference 71 (1998) 229–244.
- 337 [7] F. Ball, D. Clancy, The final size and severity of a generalised stochastic  
338 multitype epidemic model, Advances in applied probability 25 (1993)  
339 721–736.
- 340 [8] J. T. Wu, K. Leung, G. M. Leung, Nowcasting and forecasting the  
341 potential domestic and international spread of the 2019-ncov outbreak  
342 originating in wuhan, china: a modelling study, The Lancet (2020).
- 343 [9] J. M. Read, J. R. Bridgen, D. A. Cummings, A. Ho, C. P. Jewell, Novel  
344 coronavirus 2019-ncov: early estimation of epidemiological parameters  
345 and epidemic predictions, medRxiv (2020).
- 346 [10] B. Tang, X. Wang, Q. Li, N. L. Bragazzi, S. Tang, Y. Xiao, J. Wu,  
347 Estimation of the transmission risk of 2019-ncov and its implication for  
348 public health interventions, Available at SSRN 3525558 (2020).
- 349 [11] W. S. Cleveland, S. J. Devlin, Locally weighted regression: an approach  
350 to regression analysis by local fitting, Journal of the American statistical  
351 association 83 (1988) 596–610.
- 352 [12] Q. Li, X. Guan, P. Wu, X. Wang, L. Zhou, Y. Tong, R. Ren, K. S.  
353 Leung, E. H. Lau, J. Y. Wong, et al., Early transmission dynamics in  
354 wuhan, china, of novel coronavirus-infected pneumonia, New England  
355 Journal of Medicine (2020).
- 356 [13] W. Guan, Z. Ni, Y. Hu, W. Liang, C. Ou, J. He, et al., N. Zhong, Clinical  
357 characteristics of 2019 novel coronavirus infection in china, medRxiv  
358 (2020).

- 359 [14] N. Chen, M. Zhou, X. Dong, J. Qu, F. Gong, Y. Han, Y. Qiu, J. Wang,  
360 Y. Liu, Y. Wei, et al., Epidemiological and clinical characteristics of 99  
361 cases of 2019 novel coronavirus pneumonia in wuhan, china: a descrip-  
362 tive study, *The Lancet* (2020).
- 363 [15] Shenzhen Municipal Affairs Service Data Administration, Lat-  
364 est data, Available at [https://opendata.sz.gov.cn/data/dataSet/  
365 toDataSet](https://opendata.sz.gov.cn/data/dataSet/toDataSet), 2020. [Accessed February 14, 2020].
- 366 [16] Shaoyang Municipal Health Commission, Dynamic information on  
367 prevention and control of new coronavirus-infected pneumonia in  
368 shaoyang, Available at [https://wjw.shaoyang.gov.cn/wjw/zyxw/  
369 202002/c49df53092784c85aaac769149f30265.shtml](https://wjw.shaoyang.gov.cn/wjw/zyxw/202002/c49df53092784c85aaac769149f30265.shtml), 2020. [Accessed  
370 February 14, 2020].

Table 1: The reproduction number  $R_0^D$  at three infectious durations:  $D = 7, 10.5, 14$ , for the 30 mainland provinces and 15 cities in Hubei province on February 10th. The symbols + (-) indicate that the  $R_0^{14}$  was significantly above (below) 1 at 5% level of statistical significance, and the numbers inside the square brackets were the consecutive days the  $R_0^{14}$  were above or below 1. The columns headed with  $\Delta R_0$ ,  $\Delta R_0(1^{st})$  and  $\Delta R_0(2^{nd})$  are the percentages of decline in the  $R_0^{14}$  from the beginning of analysis to February 10th, to February 3rd, and the from February 3-10, respectively.

Province/City	$R_0^7$	$R_0^{10.5}$	$R_0^{14}$	$\Delta R_0$	$\Delta R_0(1^{st})$	$\Delta R_0(2^{nd})$
Ezhou	0.9-[1]	1.35+	1.8+	83.6%	78.6%	23.2%
Wuhan	0.87-[1]	1.31+	1.74+	71.2%	43.7%	48.8%
Tianmen	0.87-[6]	1.3+	1.74+	73.7%	65.1%	24.8%
Guizhou	0.87-[4]	1.3+	1.73+	62.8%	8.3%	59.4%
Hubei	0.67-[2]	1.01	1.34+	78.8%	48.9%	58.5%
Xiantao	0.65-[2]	0.97	1.3+	78.4%	44.9%	60.7%
Heilongjiang	0.63-[2]	0.95	1.26+	82.5%	53.8%	62.1%
Xinjiang	0.6-[5]	0.9-[2]	1.2+	76%	59.8%	40.4%
Hebei	0.58-[7]	0.87-[1]	1.16+	87.1%	79.6%	37%
Huangshi	0.52-[3]	0.78-[1]	1.04	79.6%	32.8%	69.6%
Anhui	0.47-[5]	0.71-[1]	0.95	89.1%	70.9%	62.6%
Shiyan	0.46-[5]	0.69-[1]	0.91	89.7%	71%	64.4%
Jiangsu	0.45-[5]	0.68-[3]	0.9	88.4%	68.2%	63.5%
Shandong	0.45-[8]	0.67-[2]	0.9	91.3%	82.9%	49%
Yichang	0.45-[6]	0.67-[3]	0.89	87.8%	56.2%	72%
Guangxi	0.44-[8]	0.66-[5]	0.88	82.2%	64.3%	50.2%
Gansu	0.43-[6]	0.65-[1]	0.87	82.2%	48.6%	65.5%
Shanxi	0.43-[5]	0.65-[3]	0.86	88.9%	66.6%	66.8%
Tianjin	0.43-[5]	0.65-[2]	0.86	84.5%	52.6%	67.3%
Xiangyang	0.42-[5]	0.63-[3]	0.84-[1]	88.6%	57.3%	73.3%
Jilin	0.41-[3]	0.62-[1]	0.83	83.5%	12.1%	81.2%
Hainan	0.41-[11]	0.62-[2]	0.82-[1]	83.3%	63.9%	53.8%
Enshizhou	0.41-[7]	0.62-[4]	0.82-[2]	82.8%	59.7%	57.2%
Xiaogan	0.39-[2]	0.59-[1]	0.79-[1]	89.3%	59.9%	73.2%
Jingzhou	0.38-[4]	0.57-[2]	0.76-[1]	89.6%	48.7%	79.7%
Neimenggu	0.38-[4]	0.56-[3]	0.75-[2]	80.5%	43.5%	65.5%
Sichuan	0.37-[7]	0.55-[5]	0.73-[3]	91.1%	77.9%	59.9%
Jiangxi	0.37-[4]	0.55-[2]	0.73-[1]	91.9%	69.2%	73.8%
Suizhou	0.35-[3]	0.53-[2]	0.7-[1]	88.2%	42.1%	79.7%

Continued on next page

**Table 1 – continued from previous page**

Province/City	$R_0^7$	$R_0^{10.5}$	$R_0^{14}$	$\Delta R_0$	$\Delta R_0(1^{st})$	$\Delta R_0(2^{nd})$
Huanggang	0.34–[4]	0.52–[3]	0.69–[1]	91.6%	58.4%	79.7%
Jingmen	0.34–[6]	0.51–[1]	0.68–[1]	92.5%	76.4%	68.2%
Henan	0.32–[4]	0.48–[2]	0.64–[1]	94.4%	77.3%	75.1%
Beijing	0.32–[6]	0.47–[4]	0.63–[1]	89.7%	60.9%	73.8%
Hunan	0.3–[5]	0.46–[3]	0.61–[2]	93.6%	74.7%	74.9%
Shaanxi	0.3–[7]	0.45–[4]	0.59–[3]	88.9%	60.3%	72.1%
Chongqing	0.29–[7]	0.44–[4]	0.58–[3]	92.1%	74.3%	69.2%
Fujian	0.27–[7]	0.41–[5]	0.55–[4]	92.4%	74.1%	70.6%
Guangdong	0.26–[5]	0.39–[3]	0.53–[2]	90.2%	51.4%	79.8%
Liaoning	0.26–[7]	0.39–[6]	0.51–[2]	91.3%	69.7%	71.2%
Xianning	0.22–[5]	0.33–[3]	0.45–[2]	87.2%	20.5%	83.9%
Shanghai	0.21–[7]	0.32–[4]	0.42–[3]	92.6%	64.2%	79.3%
Ningxia	0.2–[4]	0.3–[2]	0.4–[2]	94.5%	69.5%	81.8%
Qinghai	0.14–[5]	0.21–[4]	0.28–[4]	89.8%	-1.4%	89.9%
Yunnan	0.14–[8]	0.2–[7]	0.27–[5]	97.3%	86.5%	80.2%
Zhejiang	0.14–[8]	0.2–[4]	0.27–[3]	96.5%	76.6%	84.9%
Ave(sd)	0.42(0.19)	0.64(0.28)	0.85(0.38)	87.6%	62.6%	67%

371

Table 2: The 95% prediction intervals for the peak and ending times, and the final accumulative number of infected cases of COVID-19 epidemic in the 30 provinces based on data to Feb 13 2020 with the estimated  $\hat{\gamma}_T$ . The last column lists the total infected cases ( $I(t) + R(t)$ ) as Feb 13, 2020.

Province	Peak time	Ending time	$\hat{N}_{final}$	Current
Hubei	2/20 – 2/22	3/3/21 – 3/9/21	83972 – 92103	52388
Guangdong	2/9 – 2/9	6/24/20 – 7/15/20	1364 – 1462	1271
Zhejiang	2/7 – 2/7	6/26/20 – 7/21/20	1274 – 1344	1163
Beijing	2/11 – 2/20	7/25/20 – 9/30/20	394 – 626	374
Chongqing	2/10 – 2/10	6/13/20 – 7/18/20	602 – 738	533
Hunan	2/10 – 2/10	6/5/20 – 6/29/20	1225 – 1402	989
Guangxi	2/12 – 2/23	8/14/20 – 10/11/20	259 – 463	226
Shanghai	2/9 – 2/9	6/3/20 – 7/7/20	340 – 403	326
Jiangxi	2/14 – 2/20	9/5/20 – 10/26/20	1154 – 1455	897
Sichuan	2/14 – 2/23	9/17/20 – 11/5/20	600 – 914	461
Shandong	2/23 – 3/20	10/27/20 – 3/21/21	1079 – 2415	519

Continued on next page



**Table 2 – continued from previous page**

Province	Peak time	Ending time	$\hat{N}_{\text{final}}$	Current
Anhui	2/11 – 2/24	8/25/20 – 10/27/20	1330 – 2047	937
Fujian	2/10 – 2/10	8/10/20 – 9/16/20	313 – 418	282
Henan	2/9 – 2/9	7/12/20 – 8/7/20	1444 – 1754	1197
Jiangsu	2/15 – 2/23	7/23/20 – 10/11/20	866 – 1288	589
Hainan	2/12 – 3/9	7/3/20 – 11/19/20	175 – 512	159
Tianjin	2/13 – 3/7	5/7/20 – 10/4/20	132 – 598	122
Yunnan	2/13 – 2/15	8/3/20 – 9/3/20	178 – 244	161
Shaanxi	2/10 – 2/10	7/6/20 – 9/10/20	257 – 373	231
Heilongjiang	2/15 – 2/26	9/4/20 – 10/15/20	473 – 876	414
Liaoning	2/9 – 2/15	6/7/20 – 8/24/20	127 – 194	118
Guizhou	2/12 – 2/23	5/9/20 – 7/7/20	159 – 289	141
Jilin	2/9 – 2/10	4/11/20 – 7/3/20	89 – 98	87
Ningxia	2/13 – 3/19	4/3/20 – 10/27/20	78 – 329	67
Hebei	2/17 – 3/18	7/20/20 – 11/14/20	573 – 1558	280
Gansu	2/9 – 2/9	3/22/20 – 4/26/20	95 – 131	91
Xinjiang	2/14 – 10/19	6/7/20 – 10/3/21	79 – 8791090	66
Shanxi	2/10 – 3/10	6/20/20 – 11/27/20	138 – 431	127
Neimenggu	2/14 – 2/15	6/30/20 – 7/5/20	66 – 73	64
Qinghai	2/4 – 2/4	2/25/20 – 3/3/20	19 – 19	18
Except Hubei	2/10 – 2/17	10/18/20 – 11/05/20	17894 – 19163	11977

372

Table 3: The 95% prediction intervals for the peak and ending times, and the final accumulative number of infected cases of COVID-19 epidemic in the 30 provinces based on data to Feb 13 2020 with  $\gamma = 0.1$ . The last column lists the total infected cases ( $I(t) + R(t)$ ) as Feb 13, 2020.

Province	Peak time	Ending time	$\hat{N}_{\text{final}}$	Current
Hubei	2/14 – 2/14	6/8 – 6/10	69896 – 73460	52388
Guangdong	2/9 – 2/9	4/24 – 4/26	1341 – 1413	1271
Zhejiang	2/7 – 2/7	4/23 – 4/25	1239 – 1286	1163
Beijing	2/11 – 2/11	4/12 – 4/25	390 – 513	374
Chongqing	2/10 – 2/10	4/16 – 4/24	577 – 675	533
Hunan	2/10 – 2/10	4/25 – 5/1	1151 – 1261	989
Guangxi	2/12 – 2/12	4/9 – 4/21	247 – 310	226
Shanghai	2/9 – 2/9	4/10 – 4/14	340 – 373	326

Continued on next page

**Table 3 – continued from previous page**

Province	Peak time	Ending time	$\hat{N}_{\text{final}}$	Current
Jiangxi	2/13 – 2-13	4/25 – 4/29	1050 – 1153	897
Sichuan	2/13 – 2/13	4/18 – 4/26	537 – 617	461
Shandong	2/11 – 2/11	4/27 – 5/16	704 – 889	519
Anhui	2/11 – 2/11	4/28 – 5/6	1169 – 1360	937
Fujian	2/10 – 2/10	4/10 – 4/16	302 – 342	282
Henan	2/9 – 2/9	4/26 – 5/1	1362 – 1501	1197
Jiangsu	2/13 – 2/13	4/23 – 5/4	728 – 876	589
Hainan	2/12 – 2/12	4/4 – 4/15	172 – 225	159
Tianjin	2/12 – 2/12	4/2 – 5/11	134 – 257	122
Yunnan	2/13 – 2/13	4/5 – 4/10	172 – 192	161
Shaanxi	2/10 – 2/10	4/8 – 4/15	245 – 292	231
Heilongjiang	2/13 – 2/13	4/15 – 4/22	460 – 586	414
Liaoning	2/9 – 2/9	4/1 – 4/10	125 – 152	118
Guizhou	2/12 – 2/12	4/4 – 4/14	155 – 216	141
Jilin	2/9 – 2/9	3/27 – 3/29	89 – 95	87
Ningxia	2/13 – 2/13	3/29 – 6/2	78 – 166	67
Hebei	2/13 – 2/13	4/27 – 5/24	427 – 594	280
Gansu	2/9 – 2/9	3/26 – 4/10	94 – 124	91
Xinjiang	2/13 – 2/13	3/29 – 12/24	77 – 466	66
Shanxi	2/10 – 2/10	4/1 – 4/20	136 – 193	127
Neimenggu	2/13 – 2/13	3/26 – 3/28	65 – 73	64
Qinghai	2/4 – 2/4	3/3 – 3/7	19 – 19	18
Except Hubei	2/10 – 2/10	5/25 – 5/27	15158 – 15651	11977

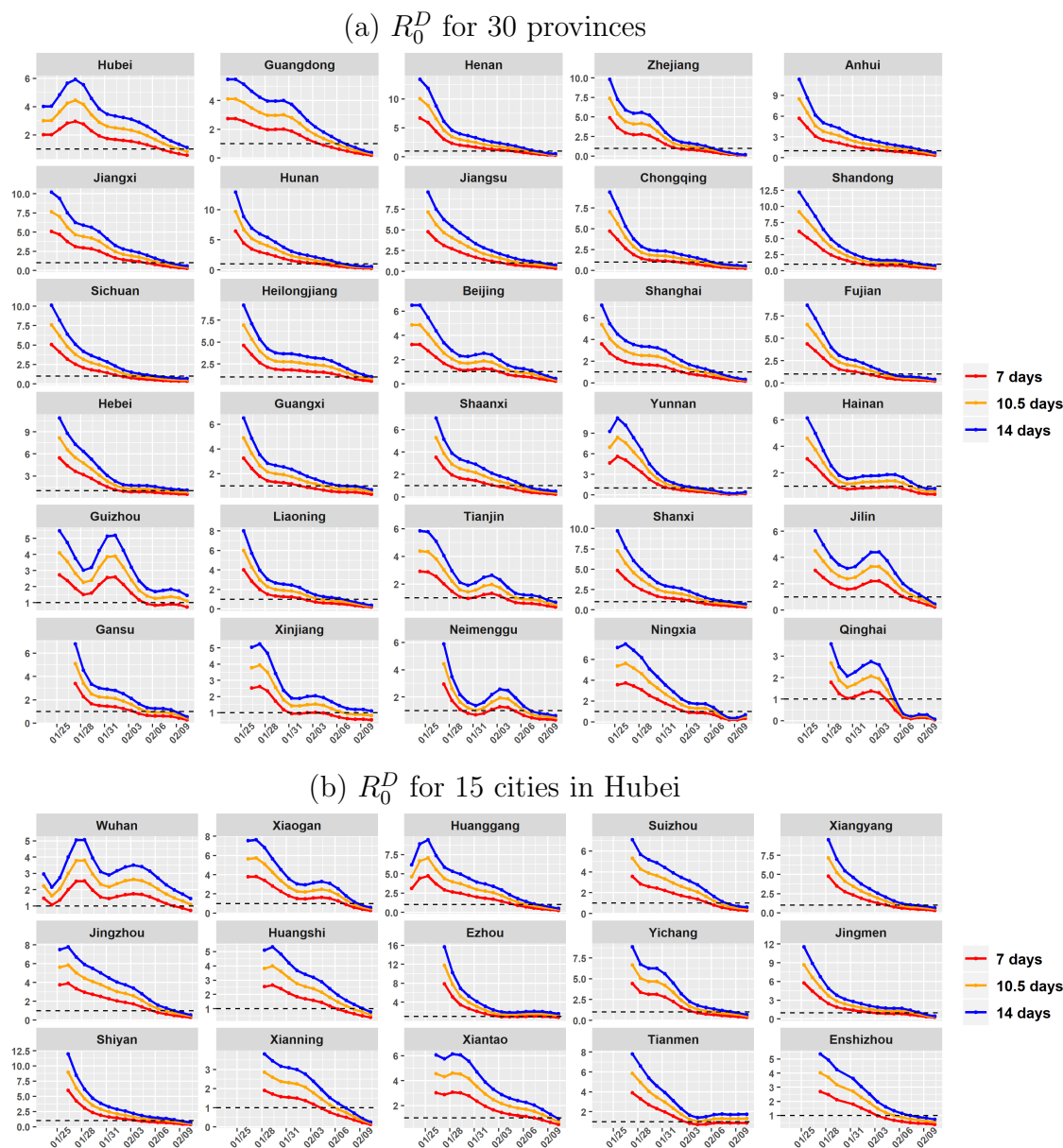


Figure 1: Time series of the reproduction number  $R_0^D(t)$  at three infectious durations:  $D = 7$  (red), 10.5 (orange), 14 (blue), for the 30 mainland provinces (a) and the 15 cities in Hubei province (b) from Jan 21 to Feb 11 2020. The black horizontal line is the critical threshold level 1.

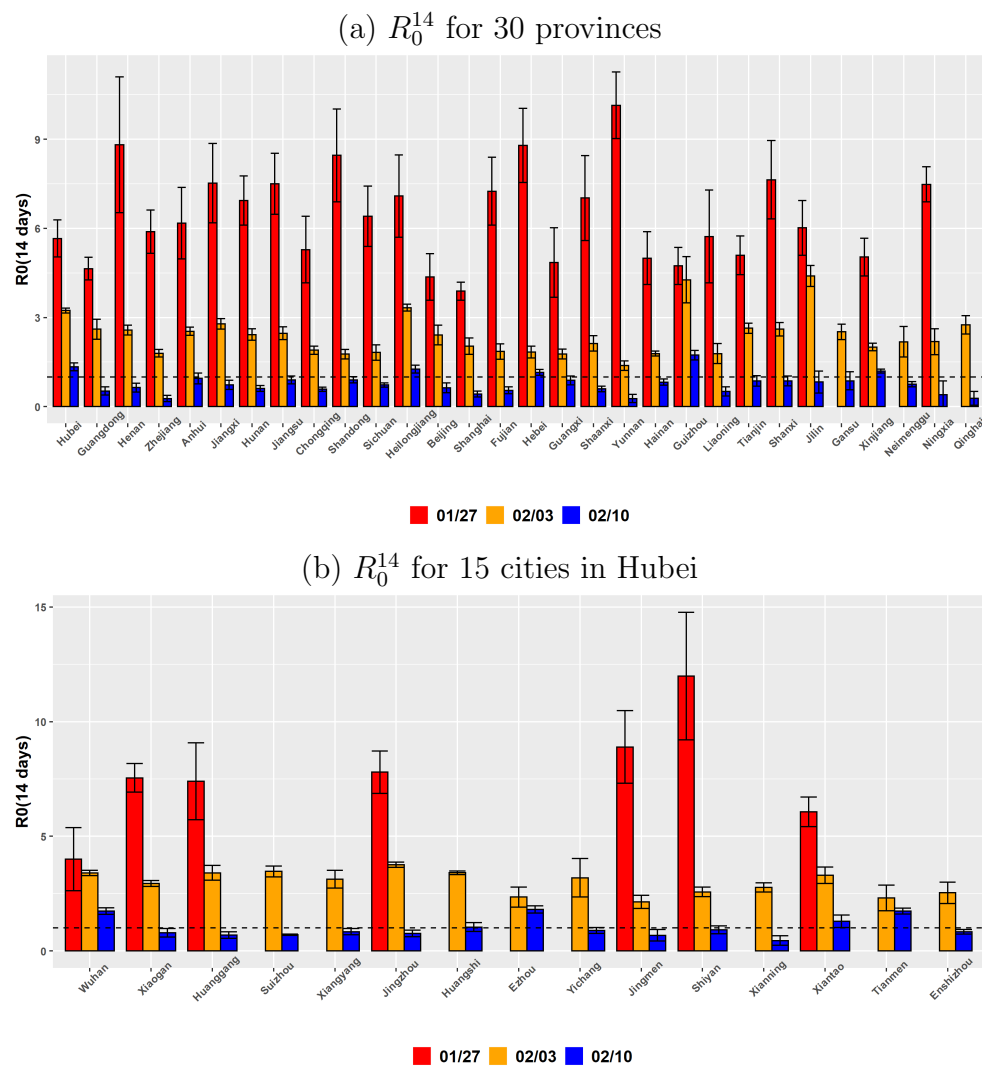


Figure 2: Elevated 95% confidence intervals (black) of the 14-day  $R_0$  for the 30 mainland provinces (a) and the 15 Hubei cities (b) on Jan 27 (red), Feb 3 (orange) and Feb 10 2020 (blue). The black horizontal lines mark the critical threshold 1.

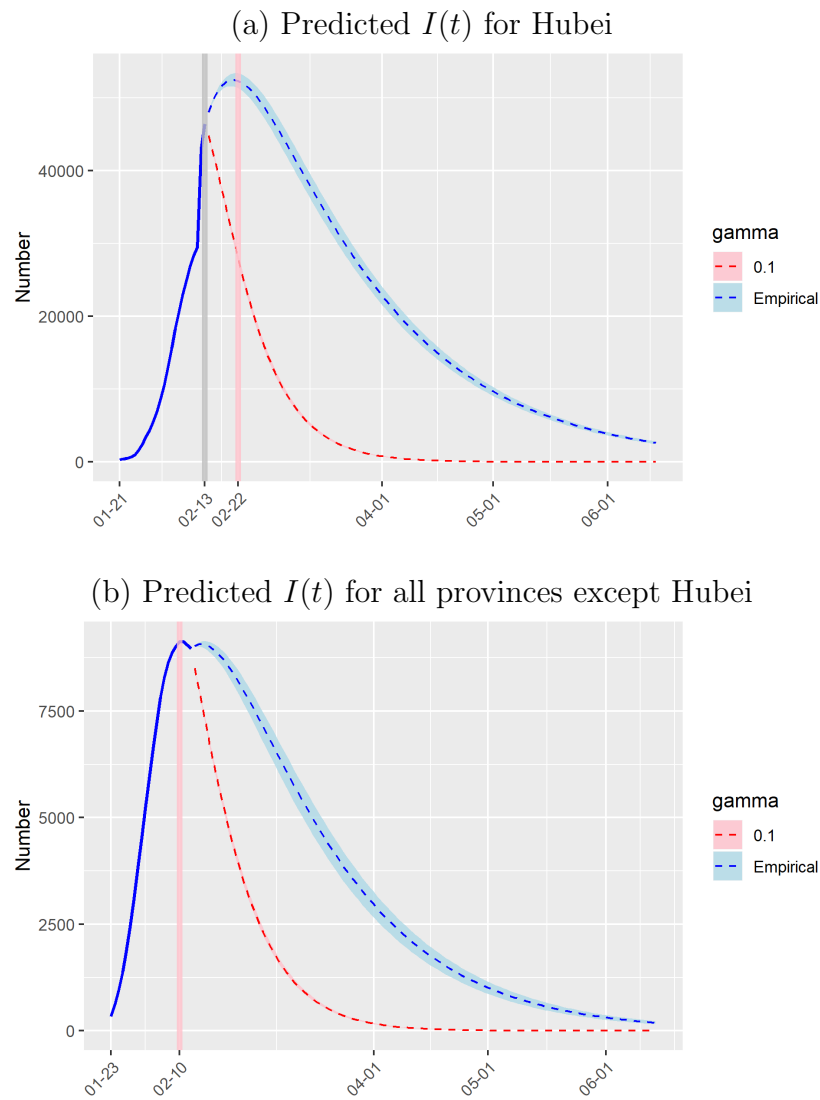


Figure 3: Predicted number of infected cases  $I(t)$  with 95% prediction interval for Hubei Province in panel (a) and all other provinces combined except Hubei in panel (b). The grey vertical line indicates the current date of observation; the blue solid line plots the observed  $I(t)$  before Feb 13th; the blue dashed line gives the predicted  $I(t)$  with 95% prediction interval (blue shaded area) with the estimated  $\hat{\gamma}_T$ ; the pink vertical line indicates the peak date of  $I(t)$ ; the red dashed line gives the predicted  $I(t)$  with 95% prediction interval (red shaded area) with fixed recovery rate  $\gamma = 0.1$ .